Redox Activated Substrates for Enhancing Activatable Cyclopropene Bioorthogonal Reactions

Wei-Siang Kao,[a] Wei Huang,[a] Yunlei Zhang,[a] Kangqiao Wen, [a] Andrea Meyer,[a] Jorge Escorihuela[b] and Scott T. Laughlin*[a]

Abstract: Bioorthogonal chemistry has become a mainstay in chemical biology and is making inroads in the clinic with recent advances in protein targeting and drug release. Since the field's beginning, a major focus has been on designing bioorthogonal reagents with good selectivity, reactivity, and stability in complex biological environments. More recently, chemists have imbued reagents with new functionalities like click-and-release or light/enzyme-controllable reactivity. We have previously developed a controllable cyclopropene-based bioorthogonal ligation, which has excellent stability in physiological conditions and can be triggered to react with tetrazines by exposure to enzymes, biologically significant small molecules, or light spanning the visual spectrum. Here, to improve reactivity and gain a better understanding of this system, we screened diene reaction partners for the cyclopropene. We found that a cyclopropene–quinone pair is 26 times faster than reactions with 1,2,4,5-tetrazines. Additionally, we showed that the reaction of the cyclopropene–quinone pair can be activated by two orthogonal mechanisms: caging group removal on the cyclopropene and oxidation/reduction of the quinone. Finally, we demonstrated that this caged cyclopropene–quinone can be used as an imaging tool to label the membranes of cultured cells.

INTRODUCTION

Since its development in the late 1990s, bioorthogonal chemistry has empowered scientists to conjugate useful chemical groups like fluorophores, biosensors, or drugs to biomolecules like proteins, lipids, and nucleic acids in cells and living organisms[1]. Many new bioorthogonal reactions have been developed, and much of the focus of bioorthogonal reagent design has been on improving reaction rates and reagent stability in the complex biological environment of living cells[2]. More recently, chemists have designed reactions with an eye towards expanded capabilities, including click-and-release for on-demand drug delivery[3] and the ability to be "turned on" by exposure to an external stimulus (*e.g.*, light, enzyme, or metabolites)[4–6]. These activatable bioorthogonal reactions provide the means to control when and where the reaction occurs, promising the ability to limit bioorthogonal reactions to specific cell types or subcellular locations, an incredibly useful feature that has been available to protein-based tools for decades. For example, Fox and coworkers have created a peroxidase- or light and photocatalyst-triggered oxidation reaction that converts dihydrotetrazine into the trans-cyclooctene-reactive s-tetrazine for reaction in hydrogels[7] and living cells[8]. While this approach takes advantage of the impressive reaction rates for trans-cyclooctene-tetrazine ligations, its use with other activation modalities has not yet been demonstrated, and the dihydrotetrazines do not quench pendant fluorophores like tetrazines, precluding the use of turn on tetrazine-fluorophores. Devaraj and coworkers have employed a similar strategy to trap the dihydrotetrazine with light labile protecting groups[9], and Mizukami and coworkers have employed a cleavable distorting chemical bridge in tetrazine to control its reaction with trans-cyclooctene[10]. Other examples include Lin and coworkers work with tetrazoles as light-activated substrates for bioorthogonal ligation via 1,3-dipolar cycloaddition[11], and Carrico and coworkers light-triggered Staudinger-Bertozzi ligation.[12]

Our work in this area has focused on the establishment of a modular enzyme-, light-, or metabolite-triggered inverse electron demand Diels–Alder (iEDDA) reaction based on the cyclopropene-tetrazine ligation **(Figure 1A)**.[13–15] In this approach, we append a caging group to a nitrogen positioned at the C3 carbon of the cyclopropene to prevent cycloaddition with s-tetrazines due to steric hindrance and modulation of the nitrogen's electron density. An advantage of this work is that the labile caging motif on the cyclopropene scaffold can be easily switched to another caging group within two steps (protecting

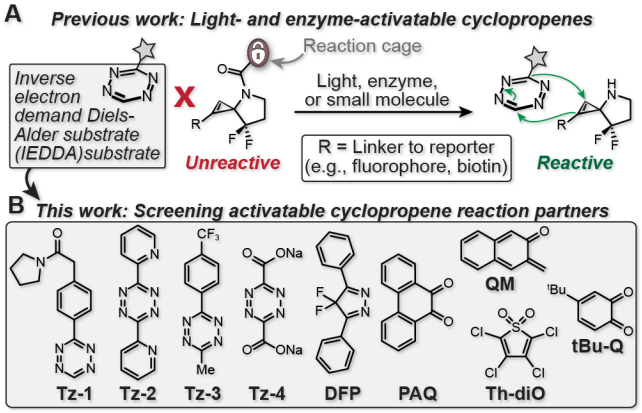

Figure 1. Potential diene substrates and strategies for reaction partner screening in activatable cyclopropene–tetrazine bioorthogonal ligations. **(A)** Previously developed activatable cyclopropene–tetrazine bioorthogonal ligation. The removal of the caging group permits the cycloaddition between cyclopropene and diene substrates like the tetrazine shown. **(B)** Diene substrates evaluated for use with activatable cyclopropenes in this work.

[a] *W.-S. Kao, W. Huang, Y. Zhang, A. Meyer, Prof. Dr. S. T. Laughlin*
Department of Chemistry, Stony Brook University
100 Nicolls Road, Stony Brook, NY 11794 (USA)
E-mail: scott.laughlin@stonybrook.edu

[b] *Prof. Dr. J. Escorihuela*
Departamento de Química Orgánica, Universitat de València, Avda. Vicente Andrés Estellés s/n, Burjassot, 46100 Valencia, Spain.

Supporting information for this article is given via a link at the end of the document.

group removal followed by caging group installation).[13] We have confirmed that the caged cyclopropene is stable under physiological conditions and in the presence of tetrazines for months without decomposing or reacting with the tetrazine. To begin the reaction, the caging group on the cyclopropene can be removed by exposure to the appropriate stimulus, such as light of the appropriate wavelength or an uncaging enzyme. Once activated, the reactions between uncaged cyclopropene and tetrazines proceed with 2nd order rate constants of $6x10^{-4}$ – $1x10^{-6}$ $M^{-1}s^{-1}$.

While we have shown that the activatable cyclopropene-tetrazine ligation can be used for bioconjugation in cells[13], optimizing the reaction kinetics to achieve parity with best-in-class bioorthogonal reagents will further improve its utility. Such optimizations can be accomplished through modifications to the cyclopropene component of the reaction, which we have explored with the creation of a ketone-containing cyclopropene[15] and continues to be of interest to our lab. Here, however, we take a different approach. We evaluate alternative iEDDA reaction partners in an effort to optimize the reaction rates of this class of activatable reaction, and, potentially, to evaluate additional activation strategies.

Essentially, we sought diene substrates that have been previously reported for other iEDDA reactions to examine whether they react with the activatable cyclopropene shown in **Figure 1A**. We began our search with modified s-tetrazines, as they are popular dienes for iEDDA reactions due to their rapid reaction rates, which can exceed 10^4 $M^{-1}s^{-1}$ with strained alkenes and alkynes.[16,17] To select compounds, we drew inspiration from recent work by Fox and coworkers exploring the commonly used preparation through a silver-mediated Liebeskind–Srogl cross-coupling.[18] This report showed that tetrazines decorated with functional groups to improve iEDDA reactivity and/or tetrazine stability could be synthesized in fewer steps than the traditional methods for tetrazine preparation.[17,19,20] In an effort to enhance the reactivity toward the dienophile, the activatable cyclopropene in our case, we selected tetrazines with strong electron withdrawing groups (**Tz-3** and **Tz-4, Figure 1B**) to evaluate whether the cycloaddition reactivity can be enhanced relative to the commonly-used tetrazines in our group and elsewhere, **Tz-1** and **Tz-2 (Figure 1B**).

In addition to tetrazines, we sought other diene substrates to evaluate as candidates for improved reactivity, each of which is shown in **Figure 1B**. These additional substrates included a 4,4-difluoro-3,5-diphenyl-4*H*-pyrazole (**DFP**, **Figure 1B**) recently reported by Raines and coworkers[21], with a 5.2 $M^{-1}s^{-1}$ reaction rate with bicyclononyne (**BCN**) that is almost two times faster than tetrazine/BCN. We also explored a 9,10-phenanthrenequinone (**PAQ**, **Figure 1B**), developed by Zhang and coworkers for visible light-triggered bioorthogonal photoclick cycloadditions. With this substrate, 405 nm light or two-photon excitation triggers the ligation with an alkene within one minute, with rate constants up to 2.76 $M^{-1}s^{-1}$.[22] We explored an *o*-naphthoquinone methide developed by Popik and coworkers (**QM**, **Figure 1B**),[23,24] which can be generated *in situ* by treating 3-(hydroxymethyl)-2-naphthol (**NQMP**) with 300 nm light (**Figure S4A**), suggesting the possibility of dual methods for controlling the bioorthogonal ligation with activatable cyclopropenes. Another substrate we evaluated was a thiophene dioxide (**Th-diO**, **Figure 1B**) developed by Wang and coworkers as a prodrug to release sulfur dioxide (SO_2) in cells after undergoing an iEDDA reaction with cyclooctyne with rates approaching 0.26 $M^{-1}s^{-1}$ in methanol at room temperature.[25] Lastly, we also evaluated a tert butyl quinone

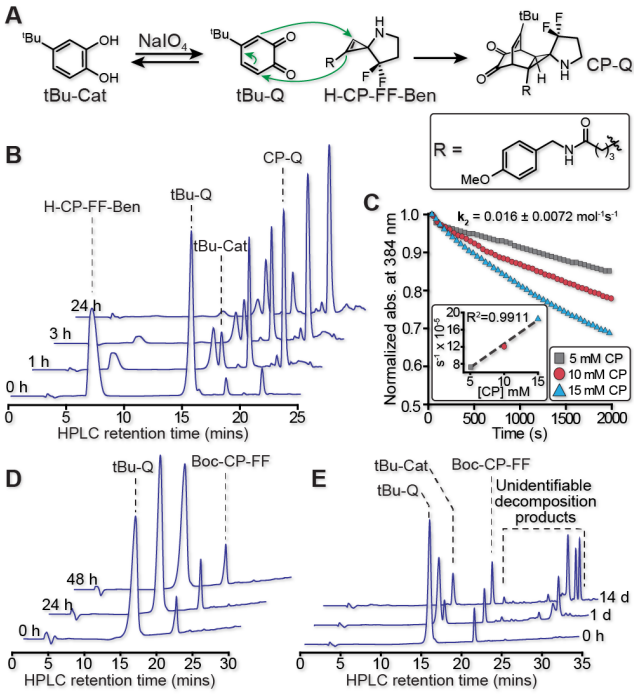

Figure 2. General bioorthogonal pairs screening process for caged-/uncaged- cyclopropene and dienes. **(A)** The cycloaddition reaction scheme of uncaged difluoro cyclopropene **H-CP-FF-Ben** and tert-butyl quinone **tBu-Q (B)** HPLC analyses of the reactivity between cyclopropene **H-CP-FF-Ben** and quinone **tBu-Q (C)** Kinetic measurement of cycloaddition rate **(D)** HPLC analyses of no reaction between caged difluoro cyclopropene **Boc-CP-FF** and tert-butyl quinone **tBu-Q** in acetonitrile **(E)** HPLC analyses of no reaction between caged cyclopropene **Boc-CP-FF** and Quinone **tBu-Q** in physiological conditions.

(**tBu-Q**, **Figure 1B**), brought to our attention by reports from Hest, van Delft, and Abhilash.[26,27] **tBu-Q**-based substrates are particularly interesting due to the potential for quinone generation *in situ* through oxidization of the corresponding catechol, raising the potential for activating the reaction by exposure to an oxidase enzyme, oxidizing agents, or light.[28]

In the following report, we describe the synthesis and evaluation of the above candidate IEDDA reaction partners for the activatable cyclopropenes. First, we determine their reactivity, stability, and synthetic accessibility. We examine the reactivity with both the caged and uncaged forms of an activatable cyclopropene (**H-CP-FF-Ben**, **Figure 2A**) as well as the stability of each diene molecule in physiological conditions. We identify one promising new reaction partner, the quinone (**tBu-Q, Figure 2A**) and then evaluate its reaction with activatable cyclopropenes in the presence or absence of an oxidant and cyclopropene activation stimulus by confocal microscopy on the membranes of cultured cells.

RESULTS AND DISCUSSION

To investigate the reactivity of an activatable cyclopropene with the candidate dienes from **Figure 1B** we used HPLC to monitor the reaction progression. First, we evaluated the modified tetrazines **Tz-3** and **Tz-4**. 1,2,4,5-Tetrazine derivatives are widely used in bioorthogonal reactions due to their fast reaction rates with cyclopropenes and trans-cyclooctenes and good selectivity at low concentrations. In previous studies, the mono-substituted tetrazine **Tz-1** and di-substituted tetrazine

Tz-2 had a second-order reaction rate of approximately 0.0006 $M^{-1}s^{-1}$ and 0.00017 $M^{-1}s^{-1}$ with difluoro-cyclopropene **H-CP-FF.**[14,15] Consistent with literature reports, we found that mono-substituted tetrazine was more reactive but less stable than di-substituted tetrazine. We predicted that introducing an electron-withdrawing group on the tetrazine would increase the reactivity towards the cyclopropene dienophile, since previous reports have suggested that the reactivity toward dienophiles may be enhanced with more electron deficient substitutions to tetrazine.[17,29–31] Accordingly, we chose **Tz-3** and **Tz-4**, which have been previously reported,[32–34] to test electron deficient tetrazines in the context of the activatable cyclopropene system.

To begin evaluating these tetrazines, we mixed **Tz-3** and **H-CP-FF-Ben** at 5 mM in 1:1 MeCN:PBS and monitored the reaction for reagent stability and product formation by HPLC. After 2 hours, we observed no change in the HPLC trace, indicating no, or very slow, reactivity with the reagent pair (**Figure S1**). Extending the reaction time to 3 days showed a small decrease in HPLC peak volume for both reagents and the formation of two small broad peaks whose identity we were unable to determine by mass spectrometry (**Figure S1**).

Moving on to **Tz-4**, early studies by Bradley and coworkers found that the Diels-Alder reaction between **Tz-4** and allyl glycidyl ether in DMSO reaches 100% conversion in ~1.5 hours.[35] Later, Koert and coworkers showed that **Tz-4** reacts with cyclooctyne in room temperature CH_2Cl_2, reaching completion in ~40 seconds.[36] However, we observed no product formation in our HPLC assay with the activatable cyclopropene **H-CP-FF-Ben**. When we tested the tetrazine **Tz-4** with cyclopropene, we found that the **Tz-4** had poor stability and decomposed quickly in aqueous buffer, producing no identifiable products according to ^{1}H NMR analysis of the reaction mixture.[31,37]

We continued our exploration of other candidate diene reaction partners with **H-CP-FF-Ben** with **DFP** (**Figure 1B**). Previous work by Raines and coworkers found a reaction rate between **DFP** and **BCN** of 5.2 $M^{-1}s^{-1}$, two times faster than **BCN** with diphenyl tetrazine in physiological conditions.[21] To test **DFP**'s reactivity toward the cyclopropene **H-CP-FF-Ben**, we performed an HPLC analysis in MeCN: PBS=1:1, monitoring reaction times as long at 24 h. Unfortunately, under these conditions we did not observe either the formation of products or decomposition of starting materials **(Figure S2)**.

Next, we moved on to evaluate **PAQ** and **QM** (**Figure 1B**) as potential reaction partners with **H-CP-FF-Ben**. Previous reports have shown that the cycloaddition between alkene and **PAQ**, or **QM**, can be initiated by light in a wavelength range of 250 to 350 nm.[22,38–40] Intrigued by the possibility of dual activation modalities (*i.e.*, light-based formation of the **PAQ** or **QM** and light- or enzyme-based activation of the cyclopropene), we investigated their reaction with **H-CP-FF-Ben**. We first examined the reaction between **H-CP-FF-Ben** and **PAQ** in the dark for 1 h. As expected for this duration in the dark, we observed no decomposition or product formation by HPLC (**Figure S3**). Unfortunately, when the mixture of **H-CP-FF-Ben** and **PAQ** was irradiated with 365 nm or 405 nm light for 1 minute to activate PAQ, we observed decomposition of cyclopropene **H-CP-FF-Ben (Figure S3).** We hypothesize that light-activated PAQ, which forms a radical intermediate upon light exposure,[22] reacted with the cyclopropene to form a mixture of unidentifiable side products. We then evaluated **QM**'s reactivity with **H-CP-FF-Ben**. In these studies, we found, consistent with literature reports,[23] that the quinone methide intermediate has a short halflife ($\tau \approx 7$ ms) in aqueous conditions, reducing back to the starting material, 3-(hydroxymethyl)-2-naphthol (**NQMP**), thus precluding its reaction with **H-CP-FF-Ben (Figure S4)**.

We then moved our attention to **Th-diO** (**Figure 1B**), which has been shown in previous reports to be a versatile substrate that can be used as an iEDDA diene.[25] Previous research has demonstrated that thiophene dioxide derivatives can undergo Diels–Alder reactions with alkynes or alkenes, followed by the release of sulfur dioxide to form the aromatic ring.[3,41] Thiophene dioxide derivatives share a similar two-step mechanism with tetrazine derivatives, where the cheletropic reaction occurs after cycloaddition between diene and dienophile. In the first step, the cycloaddition rate depends on the energy gap differences between the diene's LUMO and the dienophile's HOMO. The conformation of the product and the tendency to form the aromatic ring are the two major driving forces in the second step. To improve the reactivity and solubility in the reaction media (acetonitrile: PBS in 1:1), we selected tetrachlorothiophene dioxide **Th-diO** as the diene to analyze the ligation rate with cyclopropene. Our HPLC analyses followed a similar method to that used for the other candidate dienes described above, unfortunately, once again showing no product formation **(Figure S5)**.

Finally, we concluded our new diene reaction partner search by exploring the reaction between for **H-CP-FF-Ben** and 1,2-quinones. 1,2-quinones have been reported to undergo a concerted [4+2] cycloaddition reaction with cyclooctynes in organic solvents.[26] The 1,2-quinone can be generated by oxidizing the corresponding catechol with sodium periodate or tyrosinase to form the 1,2-quinone from phenol in the presence of oxygen (**Figure 2A**).[28] Due to their fast reaction rate with cyclooctyne, 1,2-quinone substrates have been explored as bioorthogonal diene substrates with reaction rates up to 500 $M^{-1}s^{-1}$.[26] Here, we investigated the reactivity of cyclopropene **H-CP-FF-Ben** with tert-butyl quinone **tBu-Q** in a 1-to-1 ratio in 50% acetonitrile/PBS at room temperature. Our HPLC analysis showed that the starting material cyclopropene **H-CP-FF-Ben** and tert-butyl quinone **tBu-Q**, gradually decreased in intensity and new peaks appeared over time (**Figure 2B**). We collected the three new peaks at retention times t_R = 16.4 min, 18.8 min, and 21.9 min and characterized them by NMR and high-resolution mass spectrometry. The peak at t_R = 16.4 min corresponded to the tert-butyl catechol **tBu-Cat**. Interestingly, the peak at t_R = 18.8 min initially increases and then decreases over time. This compound had a m/z of 517.3, 16 mass units more than observed for the product **CP-Q** (discussed below, m/z = 501.3), suggesting that it was an oxidation byproduct (*e.g.*, formation of an N-oxide in the presence of $NaIO_4$). More rigorous characterization of this compound was complicated by its instability: multiple HPLC runs were required to obtain sufficient material for NMR analysis, but this compound degraded on the order of 24 hours into compounds we were unable to identify by NMR with MS data that did not match CP-Q or any side, degradation, or polymerization products we could envision. Finally, at t_R = 21.9 min we observed the cycloaddition product **CP-Q**. All NMR and MS characterization data was consistent with the proposed **CP-Q** structure (*e.g.*, HRMS for **CP-Q** was found as 501.2558 which matched the calculated value). Interestingly, we observed only one diastereomer reaction product, shown in **Figure 2A**. To better understand this unexpected diastereoselectivity, we performed theoretical calculations to determine the transition state energies of the eight expected diastereomers. All cycloadditions occurred via a concerted mechanism involving a non-synchronous transition state. We identified one diastereomer with a 1.8 kcal/mol lower

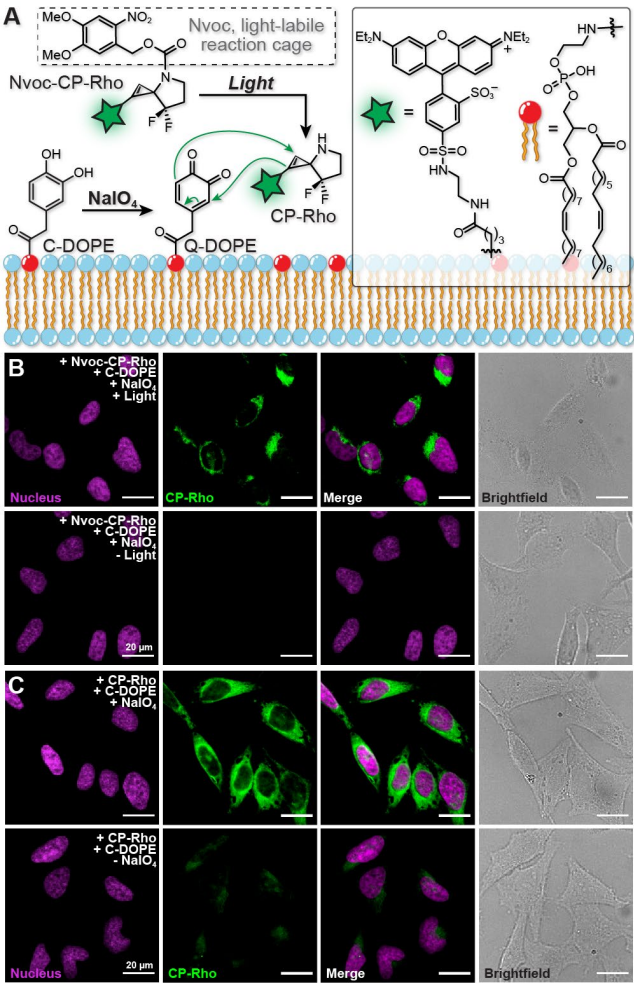

Figure 3. The light- and oxidation-activatable cyclopropene-quinone reaction for cell imaging. **(A)** Schematic description of the activatable cyclopropene-quinone system for imaging labeled lipids in cells. A catechol-labeled phospholipid (**C-DOPE**) was incubated with cells for incorporation into cellular membranes. An activatable cyclopropene caged by the light-labile Nvoc group and labeled with sulforhodamine B (**Nvoc-CP-Rho**) was then delivered to cells. Exposure to light removes Nvoc to activate the cyclopropene (**CP-Rho**) and addition of $NaIO_4$ converts C-DOPE into the reactive quinone-conjugated phospholipid (**Q-DOPE**), allow the ligation reaction to proceed. **(B)** Light- and oxidation-activated ligation for cellular imaging. Top row, the ligation reaction was initiated after 365 nm light irradiation for 1 minute. Prominent CP-Rho labeling can be observed (Green). Bottom row, without 365 nm light exposure the caged Nvoc-CP-Rho remains intact, producing no observable CP-Rho labeling. **(C)** Evaluating the requirement for oxidant exposure. Top row, with the addition of $NaIO_4$, the provided CP-Rho produced prominent fluorescent labeling of cell membranes (Green). Bottom row, without the addition of NaIO4, only minimal labeling with CP-Rho is observed. Magenta nucleus fluorescence represents Hoescht 33342 labeled nuclei. Images are displayed as maximum intensity projections of a confocal microscopy z stack. All scale bars: 20 µm

transition state energy than the next lowest diastereomer (**Figure S6**, lowest energy transition state diastereomer is shown in **Figure 2A**), suggesting that, as observed experimentally, predominantly one diastereomer would be formed in this reaction. After a day, **H-CP-FF-Ben** was consumed and only trace **tBu-Q** remained, with the majority of the reaction mixture being composed of the expected ligation product **CP-Q** and reduced **tBu-Q** in the form of **tBu-Cat**. The yield of CP-Q was 53% when the reaction was performed in 50% PBS/MeCN, and 73% when the reaction was performed in MeCN alone. We evaluated the reaction rate of this cyclopropene–quinone reaction by monitoring the disappearance of tert-butyl quinone **tBu-Q** using its characteristic absorbance at 384 nm and found a second-order rate constant of 0.016 +/- 0.0072 $M^{-1}s^{-1}$, which is 26 times faster than **H-CP-FF-Ben**'s reaction with **Tz-1 (Figure 2C)**.

Having identified a new reaction partner for this activatable cyclopropene, we next sought to confirm the cyclopropene's ability to be caged by N-modification and activated by N-modification removal. Previous studies have shown these activatable cyclopropenes can have their reactivity caged through N-modification with a diverse array of carbamate-linked removable protecting groups.[13] To evaluate reactivity caging with **tBu-Q**, we tested the reaction between a Boc-caged difluoro cyclopropene **Boc-CP-FF** and **tBu-Q** by HPLC. In these experiments, we found no reaction between these two reagents in either organic solvent **(Figure 2D)** or 50% acetonitrile/PBS buffer for over 2 weeks **(Figure 2E)**. However, we did observe **tBu-Q**'s reduction to the catechol in the 50% acetonitrile/PBS buffer conditions over 1–2 days, consistent with our results in **Figure 2B** and literature reports of quinone reduction in aqueous conditions.[42,43] We further confirmed that the new peaks are from the decomposition of tert-butyl quinone **tBu-Q** in a control experiment with only **tBu-Q** under the same 50% aqueous/organic conditions, indeed finding that the quinone is reduced to the corresponding catechol **(Figure S7)**. We did not observe this **tBu-Q** reduction in organic solvents **(Figure 2D)**.

These findings show that the reaction of quinone **tBu-Q** with uncaged activatable cyclopropene **H-CP-FF-Ben** is 26-times faster than that of the previous faster partner **Tz-1**. Additionally, the spontaneous aqueous reduction of **tBu-Q** to the catechol presents an intriguing opportunity to create a dual activatable reagent, restricting the quinone-cyclopropene reaction to cells or organelles with oxidizing environments (to generate **tBu-Q**) and further controlling reaction timing or location by light- or enzyme-based activation of a caged **H-CP-FF-Ben**.

To begin exploring the potential of this dual oxidant- and light-based reaction activation, we evaluated the activatable cyclopropene and quinone for the labeling of cellular lipids. Bioorthogonal lipid labeling has provided valuable information on lipid metabolism, localization, and lipid post-translational modifications through the incorporation of either metabolic clickable precursors or chemically synthesized lipids with clickable handles.[44–54] Nevertheless, there have been few reports for controllable bioorthogonal lipid labeling,[13,55] which would permit the use of bioorthogonal lipid labeling for studying lipid function in specific cell types or tissues. To achieve light-controllable lipid labeling, we linked the activatable difluoro cyclopropene scaffold with a sulforhodamine B fluorophore and caged it using the light-labile group Nvoc (**Nvoc-CP-Rho**) to prevent the ligation reaction from occurring prior to light exposure (**Figure 3A**). Additionally, we conjugated a catechol substrate (**tBu-Q** precursor) to a 1,2-di-(9Z-octadecenoyl)-sn-glycero-3-phosphoethanolamine (DOPE) phospholipid to obtain **C-DOPE** (**Figure 3A,** see **SI** for synthetic details and compound characterization**)**. We explored the synthesis of lipid catechols with methylene linkages (As shown in **Figure 3A**, **C-DOPE**) or more sterically hindered dimethyl substituted linkages (See SI for synthetic details). DOPE is an ethanolamine phospholipid containing two oleoyl lipid moieties. Such phospholipid ethanolamines are among the most abundant lipids in cell

membranes including both the plasma membrane and the membranes of intracellular organelles, including the ER, mitochondria, Golgi, and late endosomes[56].

We incubated Hela cells with **C-DOPE** for 1 hour to allow it to incorporate into the cell membranes. The now **C-DOPE**-labeled cells were washed three times with PBS (1 mL) and fixed with 4% PFA in PBS (1 mL) for 20 minutes at room temperature. Next, we incubated the **C-DOPE**-labeled cells with **Nvoc-CP-Rho** (10 μM in PBS) and the oxidant sodium periodate ($NaIO_4$, 1 mM in H_2O) to convert the catechols to quinones *in situ*. The chosen concentration of the oxidant sodium periodate ($NaIO_4$) was inspired by work from Francis and coworkers[28], who used it to convert an *o*-methoxy phenol into a quinone, and Paulson and coworkers[57] who used it to oxidize the cis diols of cell surface sialic acids into aldehydes for subsequent ligations. Although Francis and coworkers noted that $NaIO_4$ could also result in oxidation of cysteine and methionine sidechains, which would likely compromise cell viability, Paulson and coworkers were still able to perform $NaIO_4$ oxidation at 4 °C on living cells. Importantly, however, in this study $NaIO_4$ exposure is performed after fixation, thus mitigating any potential cell toxicity concerns. To initiate the ligation reaction, we irradiated the samples at 365 nm (1 min, 0.3W) to remove the caging group on the cyclopropene, allowing the liberated **CP-Rho** to react with **Q-DOPE** integrated into the Hela cell's membranes, or kept cells in the dark as control **(Figure 3A)**.

We then evaluated these cells by confocal microscopy. The results showed very little fluorophore labeling on the Hela cell membranes when the cyclopropene was caged in the presence of sodium periodate (**Figure 3B**, bottom panels). Once the sample was exposed to 365 nm light to release **CP-Rho**, the ligation occurred, producing clear fluorophore labeling in the cells **(Figure 3B**, top panels**)**. Notably, the subcellular distribution of the fluorescent labeling is primarily on intracellular membranes, consistent with the subcellular distributions of DOPE's PE-based phospholipid structure[56] and with the microscopy data in a previous report by Devaraj and coworkers that explored intracellular membrane labeling with DOPE-tagged bioorthogonal reagents.[44] We further examined whether adding an oxidant or light exposure would affect the ligation outcomes. Without the oxidant, the reaction produced only very modest cell membrane labeling **(Figure 3C**, bottom panels**)**, consistent with there being a small concentration of quinone produced in the absence of an added oxidizing agent. Adding $NaIO_4$ produced the expected intense fluorescent labeling of Hela cell membranes (**Figure 3C**, top panels). We also performed additional control experiments to verify that this system can only be activated by applying both light and oxidant **(Figure S8)**, and to show that prominent labeling does not occur in the presence of $NaIO_4$ but absence of **C-DOPE** (**Figure S9**). These results suggest that this catechol/quinone and activatable cyclopropene system can serve as a dual-activatable reaction for imaging cells based on the presence of an oxidizing environment, which could report on cells or organelles with oxidizing environments with the added spatiotemporal control provided by light- or enzyme-based activation of the activatable cyclopropene.

In conclusion, we have screened several classes of diene candidates in an effort to identify an activatable cyclopropene reaction partner with improved reaction rates. We found that the activatable cyclopropene **H-CP-FF-Ben** had a faster reaction rate with quinone substrates than the best-in-class tetrazines, but the quinones have poor stability in aqueous environments due to their tendency to reduce to the catechol. The addition of an oxidant served to preserve a sufficient pool of reactive quinone. Finally, we used this oxidant and light activatable reaction to image the presence of modified lipids embedded in the cell membranes of Hela cells using confocal fluorescence microscopy. The requirement of an oxidizing environment for quinine stability and efficient reaction with the activatable cyclopropene has the potential to provide a dual, *e.g.*, oxidant and light, method for reaction activation. In future studies, this dual activation approach could enable reaction activation only in highly oxidizing cell environments, *e.g.* macrophages responding to a wound or site of inflammation, and during a time period controlled by the researcher's administration of the activating light source.

Acknowledgements

We thank Nan Wang and the Center for Advanced Study of Drug Action (CASDA) at Stony Brook University for mass spectrometry resources and analysis, Dr. Francis Picart and Dr. Fang Liu for NMR instrumental support and analysis. The computational resources from the Servei d'Informàtica de la Universidad de Valencia (SIUV) are gratefully acknowledged for providing access to supercomputing resources.

Keywords: cyclopropene • bioorthogonal chemistry • click chemistry • cycloaddition

(1) E. Bird, R.; A. Lemmel, S.; Yu, X.; Angela Zhou, Q. Bioorthogonal Chemistry and Its Applications. *Bioconjug Chem* **2021**, *32* (12), 2457–2479. https://doi.org/10.1021/acs.bioconjchem.1c00461.

(2) Scinto, S. L.; Bilodeau, D. A.; Hincapie, R.; Lee, W.; Nguyen, S. S.; Xu, M.; am Ende, C. W.; Finn, M. G.; Lang, K.; Lin, Q.; Pezacki, J. P.; Prescher, J. A.; Robillard, M. S.; Fox, J. M. Bioorthogonal Chemistry. *Nature Reviews Methods Primers* **2021**, *1* (1), 30. https://doi.org/10.1038/s43586-021-00028-z.

(3) Ji, X.; Pan, Z.; Yu, B.; De La Cruz, L. K.; Zheng, Y.; Ke, B.; Wang, B. Click and Release: Bioorthogonal Approaches to "on-Demand" Activation of Prodrugs. *Chem Soc Rev* **2019**, *48* (4), 1077–1094. https://doi.org/10.1039/C8CS00395E.

(4) Kumar, P.; Laughlin, S. T. Modular Activatable Bioorthogonal Reagents.

Methods Enzymol **2019**, *622*, 153–182. https://doi.org/10.1016/BS.MIE.2019.02.007.

(5) Jiang, T.; Laughlin, S. T. Enzyme- or Light-Triggered Cyclopropenes for Bioorthogonal Ligation. In *Methods in Enzymology*; Chenoweth, D. M., Ed.; Academic Press, 2020; Vol. 641, pp 1–34. https://doi.org/https://doi.org/10.1016/bs.mie.2020.04.034.

(6) Huang, W.; Laughlin, S. T. Cell-Selective Bioorthogonal Labeling. *Cell Chem Biol* **2024**, *31* (3), 409–427. https://doi.org/10.1016/J.CHEMBIOL.2023.09.010.

(7) Zhang, H.; Trout, W. S.; Liu, S.; Andrade, G. A.; Hudson, D. A.; Scinto, S. L.; Dicker, K. T.; Li, Y.; Lazouski, N.; Rosenthal, J.; Thorpe, C.; Jia, X.; Fox, J. M. Rapid Bioorthogonal Chemistry Turn-on through Enzymatic or Long Wavelength Photocatalytic Activation of Tetrazine Ligation. *J Am Chem Soc* **2016**, *138* (18), 5978–5983. https://doi.org/10.1021/jacs.6b02168.

(8) Jemas, A.; Xie, Y.; Pigga, J. E.; Caplan, J. L.; Am Ende, C. W.; Fox, J. M. Catalytic Activation of Bioorthogonal Chemistry with Light (CABL) Enables Rapid, Spatiotemporally Controlled Labeling and No-Wash, Subcellular 3D-Patterning in Live Cells Using Long Wavelength Light. *J Am Chem Soc* **2022**, *144* (4), 1647–1662. https://doi.org/10.1021/jacs.1c10390.

(9) Liu, L.; Zhang, D.; Johnson, M.; Devaraj, N. K. Light-Activated Tetrazines Enable Precision Live-Cell Bioorthogonal Chemistry. *Nat Chem* **2022**, *14* (9), 1078–1085. https://doi.org/10.1038/s41557-022-00963-8.

(10) Novianti, I.; Kowada, T.; Mizukami, S. Clip to Click: Controlling Inverse Electron-Demand Diels–Alder Reactions with Macrocyclic Tetrazines. *Org Lett* **2022**, *24* (17), 3223–3226. https://doi.org/10.1021/ACS.ORGLETT.2C01010.

(11) An, P.; Lewandowski, T. M.; Erbay, T. G.; Liu, P.; Lin, Q. Sterically Shielded, Stabilized Nitrile Imine for Rapid Bioorthogonal Protein Labeling in Live Cells. *J Am Chem Soc* **2018**, *140* (14), 4860–4868. https://doi.org/10.1021/jacs.8b00126.

(12) Shah, L.; Laughlin, S. T.; Carrico, I. S. Light-Activated Staudinger–Bertozzi Ligation within Living Animals. *J Am Chem Soc* **2016**, *138* (16), 5186–5189. https://doi.org/10.1021/jacs.5b13401.

(13) Jiang, T.; Kumar, P.; Huang, W.; Kao, W.-S.; Thompson, A. O.; Camarda, F. M.; Laughlin, S. T. Modular Enzyme- and Light-Based Activation of Cyclopropene–Tetrazine Ligation. *ChemBioChem* **2019**, *20* (17), 2222–2226. https://doi.org/10.1002/cbic.201900137.

(14) Kumar, P.; Jiang, T.; Li, S.; Zainul, O.; Laughlin, S. T. Caged Cyclopropenes for Controlling Bioorthogonal Reactivity. *Org Biomol Chem* **2018**, *16* (22), 4081–4085. https://doi.org/10.1039/C8OB01076E.

(15) Kumar, P.; Zainul, O.; Camarda, F. M.; Jiang, T.; Mannone, J. A.; Huang, W.; Laughlin, S. T. Caged Cyclopropenes with Improved Tetrazine Ligation Kinetics. *Org Lett* **2019**, *21* (10), 3721–3725. https://doi.org/10.1021/acs.orglett.9b01177.

(16) Oliveira, B. L.; Guo, Z.; Bernardes, G. J. L. Inverse Electron Demand

Diels–Alder Reactions in Chemical Biology. *Chem Soc Rev* **2017**, *46* (16), 4895–4950. https://doi.org/10.1039/C7CS00184C.

(17) Taylor, M. T.; Blackman, M. L.; Dmitrenko, O.; Fox, J. M. Design and Synthesis of Highly Reactive Dienophiles for the Tetrazine–Trans-Cyclooctene Ligation. *J Am Chem Soc* **2011**, *133* (25), 9646–9649. https://doi.org/10.1021/ja201844c.

(18) Lambert, W. D.; Fang, Y.; Mahapatra, S.; Huang, Z.; am Ende, C. W.; Fox, J. M. Installation of Minimal Tetrazines through Silver-Mediated Liebeskind–Srogl Coupling with Arylboronic Acids. *J Am Chem Soc* **2019**, *141* (43), 17068–17074. https://doi.org/10.1021/jacs.9b08677.

(19) Cañeque, T.; Müller, S.; Rodriguez, R. Visualizing Biologically Active Small Molecules in Cells Using Click Chemistry. *Nature Reviews Chemistry 2018 2:9* **2018**, *2* (9), 202–215. https://doi.org/10.1038/s41570-018-0030-x.

(20) Devaraj, N. K.; Weissleder, R.; Hilderbrand, S. A. Tetrazine-Based Cycloadditions: Application to Pretargeted Live Cell Imaging. *Bioconjug Chem* **2008**, *19* (12), 2297–2299. https://doi.org/10.1021/bc8004446.

(21) Levandowski, B. J.; Abularrage, N. S.; Houk, K. N.; Raines, R. T. Hyperconjugative Antiaromaticity Activates 4 H-Pyrazoles as Inverse-Electron-Demand Diels-Alder Dienes. *Org Lett* **2019**, *21* (20), 8492–8495. https://doi.org/10.1021/ACS.ORGLETT.9B03351/SUPPL_FILE/OL9B03351_SI_001.PDF.

(22) Li, J.; Kong, H.; Huang, L.; Cheng, B.; Qin, K.; Zheng, M.; Yan, Z.; Zhang, Y. Visible Light-Initiated Bioorthogonal Photoclick Cycloaddition. *J Am Chem Soc* **2018**, *140* (44), 14542–14546. https://doi.org/10.1021/jacs.8b08175.

(23) Arumugam, S.; Popik, V. V. Patterned Surface Derivatization Using Diels-Alder Photoclick Reaction. *J Am Chem Soc* **2011**, *133* (39), 15730–15736. https://doi.org/10.1021/JA205652M/SUPPL_FILE/JA205652M_SI_001.PDF.

(24) Arumugam, S.; Popik, V. V. Attach, Remove, or Replace: Reversible Surface Functionalization Using Thiol-Quinone Methide Photoclick Chemistry. *J Am Chem Soc* **2012**, *134* (20), 8408–8411. https://doi.org/10.1021/JA302970X/SUPPL_FILE/JA302970X_SI_001.PDF.

(25) Wang, W.; Ji, X.; Du, Z.; Wang, B. Sulfur Dioxide Prodrugs: Triggered Release of SO2via a Click Reaction. *Chemical Communications* **2017**, *53* (8), 1370–1373. https://doi.org/10.1039/C6CC08844A.

(26) Borrmann, A.; Fatunsin, O.; Dommerholt, J.; Jonker, A. M.; Löwik, D. W. P. M.; van Hest, J. C. M.; van Delft, F. L. Strain-Promoted Oxidation-Controlled Cyclooctyne–1,2-Quinone Cycloaddition (SPOCQ) for Fast and Activatable Protein Conjugation. *Bioconjug Chem* **2015**, *26* (2), 257–261. https://doi.org/10.1021/bc500534d.

(27) Nair, V.; Menon, R. S.; Biju, A. T.; Abhilash, K. G. 1,2-Benzoquinones in Diels–Alder Reactions, Dipolar Cycloadditions, Nucleophilic Additions, Multicomponent Reactions and More. *Chem Soc Rev* **2012**, *41* (3), 1050–1059. https://doi.org/10.1039/C1CS15186J.

(28) Marmelstein, A. M.; Lobba, M. J.; Mogilevsky, C. S.; Maza, J. C.; Brauer, D. D.; Francis, M. B.

Tyrosinase-Mediated Oxidative Coupling of Tyrosine Tags on Peptides and Proteins. *J Am Chem Soc* **2020**, *142* (11), 5078–5086. https://doi.org/10.1021/jacs.9b12002.

(29) Siegl, S. J.; Vázquez, A.; Dzijak, R.; Dračínský, M.; Galeta, J.; Rampmaier, R.; Klepetářová, B.; Vrabel, M. Design and Synthesis of Aza-Bicyclononene Dienophiles for Rapid Fluorogenic Ligations. *Chemistry – A European Journal* **2018**, *24* (10), 2426–2432. https://doi.org/10.1002/CHEM.201705188.

(30) Novianti, I.; Kowada, T.; Mizukami, S. Clip to Click: Controlling Inverse Electron-Demand Diels-Alder Reactions with Macrocyclic Tetrazines. *Org Lett* **2022**, *24* (17), 3223–3226. https://doi.org/10.1021/ACS.ORGLETT.2C01010.

(31) Wei, T.; Zhu, W.; Zhang, X.; Li, Y.-F.; Xiao, H. Molecular Design of 1,2,4,5-Tetrazine-Based High-Energy Density Materials. *J Phys Chem A* **2009**, *113* (33), 9404–9412. https://doi.org/10.1021/jp902295v.

(32) Denk, C.; Svatunek, D.; Mairinger, S.; Stanek, J.; Filip, T.; Matscheko, D.; Kuntner, C.; Wanek, T.; Mikula, H. Design, Synthesis, and Evaluation of a Low-Molecular-Weight 11C-Labeled Tetrazine for Pretargeted PET Imaging Applying Bioorthogonal in Vivo Click Chemistry. *Bioconjug Chem* **2016**, *27* (7), 1707–1712. https://doi.org/10.1021/acs.bioconjchem.6b00234.

(33) Sauer, J.; Bäuerlein, P.; Ebenbeck, W.; Gousetis, C.; Sichert, H.; Troll, T.; Utz, F.; Wallfahrer, U. [4+2] Cycloadditions of 1,2,4,5-Tetrazines and Cyclopropenes − Synthesis of 3,4-Diazanorcaradienes and Tetracyclic Aliphatic Azo Compounds. *European J Org Chem* **2001**, *2001* (14), 2629–2638. https://doi.org/https://doi.org/10.1002/1099-0690(200107)2001:14<2629::AID-EJOC2629>3.0.CO;2-2.

(34) R. Karver, M.; Weissleder, R.; A. Hilderbrand, S. Synthesis and Evaluation of a Series of 1,2,4,5-Tetrazines for Bioorthogonal Conjugation. *Bioconjug Chem* **2011**, *22* (11), 2263–2270. https://doi.org/10.1021/bc200295y.

(35) Jain, S.; Neumann, K.; Zhang, Y.; Geng, J.; Bradley, M. Tetrazine-Mediated Postpolymerization Modification. *Macromolecules* **2016**, *49* (15), 5438–5443. https://doi.org/10.1021/ACS.MACROMOL.6B00867/SUPPL_FILE/MA6B00867_SI_001.PDF.

(36) Meinecke, J.; Koert, U. Copper-Free Click Reaction Sequence: A Chemoselective Layer-by-Layer Approach. *Org Lett* **2019**, *21* (18), 7609–7612. https://doi.org/10.1021/acs.orglett.9b02891.

(37) V. Sadasivam, D.; Prasad, E.; A. Flowers, R.; M. Birney, D. Stopped-Flow Kinetics of Tetrazine Cycloadditions; Experimental and Computational Studies toward Sequential Transition States. *J Phys Chem A* **2005**, *110* (4), 1288–1294. https://doi.org/10.1021/jp0534075.

(38) Škalamera, D.; Mlinarić-Majerski, K.; Martin Kleiner, I.; Kralj, M.; Oake, J.; Wan, P.; Bohne, C.; Basarić, N. Photochemical Formation of Anthracene Quinone Methide Derivatives. *Journal of Organic Chemistry* **2017**, *82* (12), 6006–6021. https://doi.org/10.1021/ACS.JOC.6B02735/SUPPL_FILE/JO6B02735_SI_001.PDF.

(39) Minard, A.; Liano, D.; Wang, X.; Di Antonio, M. The Unexplored Potential of Quinone Methides in Chemical Biology. *Bioorg Med*

Chem **2019**, *27* (12), 2298–2305. https://doi.org/https://doi.org/10.1016/j.bmc.2019.04.001.

(40) Li, Q.; Dong, T.; Liu, X.; Lei, X. A Bioorthogonal Ligation Enabled by Click Cycloaddition of O-Quinolinone Quinone Methide and Vinyl Thioether. *J Am Chem Soc* **2013**, *135* (13), 4996–4999. https://doi.org/10.1021/JA401989P/SUPPL_FILE/JA401989P_SI_001.PDF.

(41) Meguro, T.; Yoshida, S.; Hosoya, T. Sequential Molecular Conjugation Using Thiophene S,S-Dioxides Bearing a Clickable Functional Group. *Chem Lett* **2017**, *46* (8), 1137–1140. https://doi.org/10.1246/cl.170426.

(42) T. Huynh, M.; W. Anson, C.; C. Cavell, A.; S. Stahl, S.; Hammes-Schiffer, S. Quinone 1 e– and 2 e–/2 H+ Reduction Potentials: Identification and Analysis of Deviations from Systematic Scaling Relationships. *J Am Chem Soc* **2016**, *138* (49), 15903–15910. https://doi.org/10.1021/jacs.6b05797.

(43) Gupta, N.; Linschitz, H. Hydrogen-Bonding and Protonation Effects in Electrochemistry of Quinones in Aprotic Solvents. *J Am Chem Soc* **1997**, *119* (27), 6384–6391. https://doi.org/10.1021/ja970028j.

(44) Yang, J.; Šečkute, J.; Cole, C. M.; Devaraj, N. K. Live-Cell Imaging of Cyclopropene Tags with Fluorogenic Tetrazine Cycloadditions. *Angewandte Chemie International Edition* **2012**, *51* (30), 7476–7479. https://doi.org/10.1002/ANIE.201202122.

(45) Peng, T.; Hang, H. C. Bifunctional Fatty Acid Chemical Reporter for Analyzing S-Palmitoylated Membrane Protein-Protein Interactions in Mammalian Cells. *J Am Chem Soc* **2015**, *137* (2), 556–559. https://doi.org/10.1021/JA502109N/SUPPL_FILE/JA502109N_SI_003.XLSX.

(46) Won, S. J.; Martin, B. R. Temporal Profiling Establishes a Dynamic S-Palmitoylation Cycle. *ACS Chem Biol* **2018**, *13* (6), 1560–1568. https://doi.org/10.1021/ACSCHEMBIO.8B00157/SUPPL_FILE/CB8B00157_SI_007.XLSX.

(47) Thinon, E.; Hang, H. C. Chemical Reporters for Exploring Protein Acylation. *Biochem Soc Trans* **2015**, *43* (2), 253–261. https://doi.org/10.1042/BST20150004.

(48) Davda, D.; El Azzouny, M. A.; Tom, C. T. M. B.; Hernandez, J. L.; Majmudar, J. D.; Kennedy, R. T.; Martin, B. R. Profiling Targets of the Irreversible Palmitoylation Inhibitor 2-Bromopalmitate. *ACS Chem Biol* **2013**, *8* (9), 1912–1917. https://doi.org/10.1021/CB400380S/SUPPL_FILE/CB400380S_SI_002.PDF.

(49) Gao, X.; Hannoush, R. N. A Decade of Click Chemistry in Protein Palmitoylation: Impact on Discovery and New Biology. *Cell Chem Biol* **2018**, *25* (3), 236–246. https://doi.org/10.1016/J.CHEMBIOL.2017.12.002.

(50) Ngo, J. T.; Adams, S. R.; Deerinck, T. J.; Boassa, D.; Rodriguez-Rivera, F.; Palida, S. F.; Bertozzi, C. R.; Ellisman, M. H.; Tsien, R. Y. Click-EM for Imaging Metabolically Tagged Nonprotein Biomolecules. *Nature Chemical Biology 2016 12:6* **2016**, *12* (6), 459–465. https://doi.org/10.1038/nchembio.2076.

(51) Wang, D.; Du, S.; Cazenave-Gassiot, A.; Ge, J.; Lee, J.-S.; Wenk, M. R.; Yao, S. Q. Global Mapping of Protein–Lipid Interactions by Using Modified Choline-Containing Phospholipids Metabolically Synthesized in Live Cells.

Angewandte Chemie **2017**, *129* (21), 5923–5927. https://doi.org/10.1002/ANGE.201702509.

(52) Bumpus, T. W.; Baskin, J. M. A Chemoenzymatic Strategy for Imaging Cellular Phosphatidic Acid Synthesis. *Angewandte Chemie International Edition* **2016**, *55* (42), 13155–13158. https://doi.org/10.1002/ANIE.201607443.

(53) Walter, A. M.; Müller, R.; Tawfik, B.; Wierda, K. D.; Pinheiro, P. S.; Nadler, A.; McCarthy, A. W.; Ziomkiewicz, I.; Kruse, M.; Reither, G.; Rettig, J.; Lehmann, M.; Haucke, V.; Hille, B.; Schultz, C.; Sørensen, J. B. Phosphatidylinositol 4,5-Bisphosphate Optical Uncaging Potentiates Exocytosis. *Elife* **2017**, *6*. https://doi.org/10.7554/ELIFE.30203.

(54) Jao, C. Y.; Roth, M.; Welti, R.; Salic, A. Metabolic Labeling and Direct Imaging of Choline Phospholipids in Vivo. *Proc Natl Acad Sci U S A* **2009**, *106* (36), 15332–15337. https://doi.org/10.1073/PNAS.0907864106/SUPPL_FILE/0907864106SI.PDF.

(55) Kumar, P.; Jiang, T.; Zainul, O.; Preston, A. N.; Li, S.; Farr, J. D.; Suri, P.; Laughlin, S. T. Lipidated Cyclopropenes via a Stable 3-N Spirocyclopropene Scaffold. *Tetrahedron Lett* **2018**, *59* (37), 3435–3438. https://doi.org/https://doi.org/10.1016/j.tetlet.2018.08.010.

(56) Van Meer, G.; Voelker, D. R.; Feigenson, G. W. Membrane Lipids: Where They Are and How They Behave. *Nature Reviews Molecular Cell Biology 2008 9:2* **2008**, *9* (2), 112–124. https://doi.org/10.1038/nrm2330.

(57) Zeng, Y.; Ramya, T. N. C.; Dirksen, A.; Dawson, P. E.; Paulson, J. C. High-Efficiency Labeling of Sialylated Glycoproteins on Living Cells. *Nature Methods 2009 6:3* **2009**, *6* (3), 207–209. https://doi.org/10.1038/nmeth.1305.

Entry for the Table of Contents (Please choose one layout)

Layout 1:

COMMUNICATION

Text for Table of Contents

((Insert TOC Graphic here))

*Author(s), Corresponding Author(s)**

Page No. – Page No.

Title

Layout 2:

COMMUNICATION

((Insert TOC Graphic here))

*Author(s), Corresponding Author(s)**

Page No. – Page No.

Title

Text for Table of Contents